HUNGARIAN JOURNAL OF
INDUSTRY AND CHEMISTRY
Vol. 54(1) pp. 43–48 (2026)
hjic.mk.uni-pannon.hu
DOI: 10.33927/hjic-2026-06

EFFECT OF CO-LIGANDS ON THE H_2O_2-OXIDATION OF 2-PHENYLPROPIONALDEHYDE CATALYZED BY NON-HEME IRON CATALYSTS AS BIOMIMICS

PATRIK TÖRÖK[1], BÁLINT VINCZE[1] AND JÓZSEF KAIZER[1]*

1 Research Group of Bioorganic and Biocoordination Chemistry, University of Pannonia, Egyetem u. 10, Veszprém, 8200, HUNGAR

In this study, the effect of various co-ligands on the reactivity of iron-based catalytic systems toward the oxidation of 2-phenylpropionaldehyde (PPA) was investigated. The oxidations were carried out in the presence of hydrogen peroxide (H_2O_2) as the terminal oxidant. The reactivity of the catalytic species was found to strongly depend on the electronic and steric properties of the applied co-ligands. By varying the co-ligand environment, significant changes were observed in both the reaction rate and product distribution, indicating that the coordination sphere around the iron center plays a key role in modulating the catalytic behavior. These findings highlight the importance of ligand effects in tuning the selectivity and efficiency of H_2O_2-driven oxidation reactions of aldehydes.

Keywords: non-heme iron, catalysis, oxidation, aldehyde

1. Introduction

Non-heme iron complexes are widely used as biomimetic model compounds to explore the mechanisms of metalloenzymes that catalyze a variety of oxidative transformations [1]-[6]. In these systems, hydrogen peroxide (H_2O_2) is frequently employed as an oxidant, leading to the in situ formation of high-valent iron-*oxo* or *μ-peroxo*-diiron(III) intermediates. These reactive species are capable of mediating challenging oxidation reactions, including C–H bond activation, deformylation and hydroxylation processes [7]-[10]. Their reactivity and selectivity are highly sensitive to the coordination environment around the metal center, particularly the electronic and steric properties of the co-ligands.

Recent studies have shown that subtle changes in equatorial or axial co-ligands can significantly affect the redox properties, stability and nucleophilic-electrophilic nature of intermediates, thereby influencing the reaction outcome and product distribution 0,[12].

Building on these results, our previous work revealed clear correlations between the Fe(III)/Fe(II) redox potentials and the rates of aldehyde deformylation reactions mediated by *μ-1,2-peroxo*-diiron(III) complexes [13].

In the present study, the H_2O_2-oxidation of 2-phenylpropionaldehyde (PPA) catalyzed by non-heme iron catalysts as synthetic enzyme models is addressed. By employing various monodentate nitrogen donor co-ligands, how the electronic characteristics of the ligand sphere affect the catalytic performance is investigated.

The relationship between structure and reactivity is explored through kinetic and spectroscopic studies, providing further insights into the role of co-ligands in tuning the efficiency as well as selectivity of non-heme iron-catalyzed oxidation reactions.

2. Experimental

The ligand (PBI: 2-(2-pyridyl)benzimidazole) as well as the substrate (PPA: 2-phenylpropionaldehyde) were purchased from Aldrich Chemical Company and used without further purification. Solvents were purified by standard procedures, distilled and stored under an Ar atmosphere over 4 Å molecular sieves. The complex $[Fe(PBI)_3](OTf)_2$ was synthesized and characterized according to a method in the literature [13].

UV-Vis measurements were carried out by an Agilent 8453 diode array UV-Visible spectrophotometer, operated with Agilent ChemStation software (2002). The samples were transferred into quartz cells prior to taking measurements. The temperature was controlled by a thermostat.

Cyclic voltammetry measurements were taken by an SP-150 potentiostat. Data were evaluated using the EC-Lab V11.41 software. A three-electrode arrangement was used to measure the potentials with the working electrode being a 3.0 mm-diameter glassy carbon

Received: 2 Oct 2025; Revised: 4 Oct 2025;
Accepted: 6 Oct 2025
*Correspondence: kaizer.jozsef@mk.uni-pannon.hu

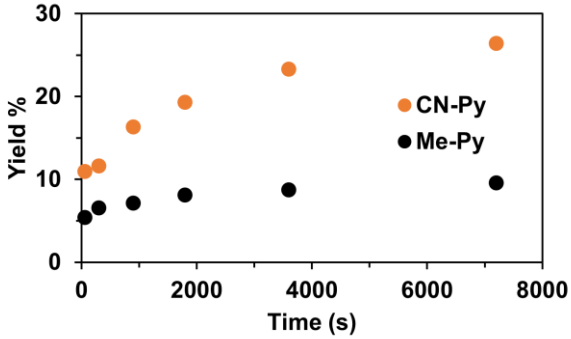

Figure 1: Time-dependent oxidation yields of 2-phenylpropionaldehyde in the presence of $[Fe(PBI)_3](OTf)_2$ using 4-cyanopyridine (CN-Py, orange) and 4-methylpyridine (Me-Py, black) as co-ligands under identical conditions (293 K, $[complex]_0 = 1.0\times10^{-3}$ M, $[co\text{-}ligand]_0 = 10.0\times10^{-3}$ M, $[PPA]_0 = 300.0\times10^{-3}$ M, $[H_2O_2]_0 = 100.0\times10^{-3}$ M)

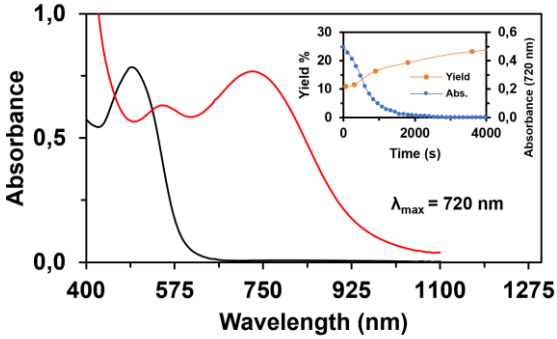

Figure 2: Correlation between catalytic activity and intermediate decay during the H_2O_2-oxidation of 2-phenylpropionaldehyde using $[Fe(PBI)_3](OTf)_2$ with 4-cyanopyridine as a co-ligand at 293 K ($[complex]_0 = 1.0\times10^{-3}$ M, $[co\text{-}ligand]_0 = 10.0\times10^{-3}$ M, $[PPA]_0 = 300.0\times10^{-3}$ M, $[H_2O_2]_0 = 100.0\times10^{-3}$ M); Product yield (orange) and absorbance decrease at 720 nm (blue) as a function of time

electrode. A Pt wire was used as the counter electrode and an Ag/Ag^+ (1M tetrabutylammonium perchlorate in acetonitrile) electrode was used as the reference electrode. The supporting electrolyte was 0.1 M tetrabutylammonium perchlorate.

Gas chromatography (GC) and mass spectrometry (GC-MS) measurements were carried out using an Agilent 7820A gas chromatograph with a 30 m Equity-1 capillary GC column equipped with a flame ionization detector as well as a Shimadzu QP2010 SE mass spectrometer equipped with a secondary electron multiplier detector including a conversion dynode and a 30 m HP-5MS GC column.

Catalytic reactions were followed by UV-Vis spectrophotometry: A stock solution of $[Fe(PBI)_3](OTf)_2$ was made in acetonitrile (1.0×10^{-3} M). 3 ml of the complex solution, co-ligand (10.0×10^{-3} M) and 2-phenylpropionaldehyde (300.0×10^{-3} M) was added to a quartz cell. The temperature was set to 293 K and H_2O_2 (100.0×10^{-3} M) was added to the solution. The reaction was monitored by following the changes in absorbance at 720 nm. The reaction rates were calculated using Agilent ChemStation software.

Catalytic oxidations: A stock solution of $[Fe(PBI)_3](OTf)_2$ was made in acetonitrile (1.0×10^{-3} M). 3 ml of the complex solution, co-ligand (10.0×10^{-3} M) and 2-phenylpropionaldehyde (300.0×10^{-3} M) was added to a vial. A solution of H_2O_2 was added slowly by a syringe to the reaction mixture. The solution was stirred at 293 K for 2 hours. The products were identified by GC-MS and the yields calculated based on GC using bromobenzene as an internal standard. The relative reaction rates were calculated according to the following equation:

$$k_{rel} = \frac{\log(\frac{c_1}{c_0})}{\log(\frac{c_{1H}}{c_{0H}})} \quad (1),$$

where c_0 denotes the initial concentration of PPA and c_1 represents the concentration of PPA at the end of the experiment.

The products of the oxidation of 2-phenylpropionaldehyde:

1-Phenylethanol:

(m/z) relative intensity 39.05 (11.21); 43.05 (36.92); 50.05 (14.59); 51.05 (28.80); 52.05 (7.46); 53.35 (7.38); 77.05 (56.94); 78.10 (20.19); 79.05 (100.00); 80.05 (5.89); 105.10 (7.60); 107.05 (81.56); 108.10 (6.71); 122.10 (M^+, 25.20).

Acetophenone:

(m/z) relative intensity 39.05 (7.32); 43.05 (18.31); 50.05 (18.10); 51.05 (40.12); 77.05 (90.58); 78.05 (9.17); 105.05 (100.00); 106.10 (7.55); 120.05 (M^+, 24.34).

2-Phenylpropionaldehyde:

(m/z) relative intensity 39.05 (9.23); 51.05 (15.99); 77.05 (28.37); 78.05 (9.31); 79.05 (28.83); 91.10 (11.70); 103.05 (16.39); 105.10 (100.00); 106.10 (12.32); 134.1 (M^+, 8.64).

3. Results and analysis

The catalytic oxidation of 2-phenylpropionaldehyde (PPA) with H_2O_2 in the presence of $[Fe(PBI)_3](OTf)_2$ was first investigated under time-dependent conditions to establish the optimal reaction parameters (*Figure 1*). Monitoring the reaction by UV-Vis spectroscopy revealed a characteristic absorption band at 720 nm, which decreased in intensity as the oxidation progressed. This absorption feature is characteristic of *μ-1,2-peroxo*-diiron(III) species and provides strong evidence for a metal-based catalytic pathway in which *peroxo* formation is the key step. This decrease in absorbance correlated well with the increase in product yield (*Figure 2*), confirming that the intermediate detected at 720 nm represents a catalytically relevant species. Based on these observations, the conditions applied in

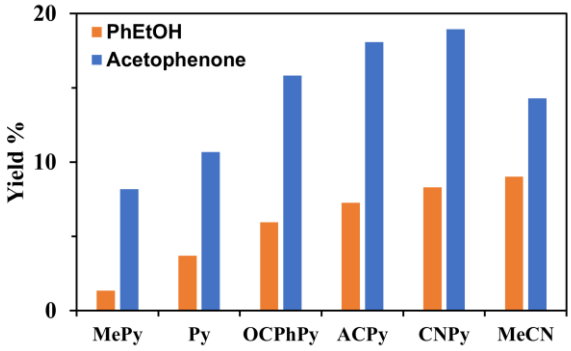

Figure 3: Effect of co-ligands on the catalytic oxidation of 2-phenylpropionaldehyde (PPA) with H_2O_2 catalyzed by $[Fe(PBI)_3](OTf)_2$ in acetonitrile at 293 K

Reaction conditions: $[Fe(PBI)_3](OTf)_2 = 1.0 \times 10^{-3}$ M, [co-ligand] = 10.0×10^{-3} M, [PPA] = 300.0×10^{-3} M, $[H_2O_2] = 100.0 \times 10^{-3}$ M
Product yields were determined by GC using bromobenzene as an internal standard.

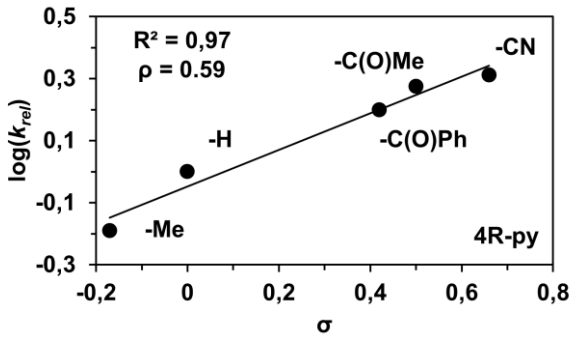

Figure 4: Hammett correlation for the H_2O_2-oxidation of 2-phenylpropionaldehyde catalyzed by $[Fe(PBI)_3](OTf)_2$ with *para*-substituted pyridine co-ligands (4R-py) at 293 K

further experiments (293 K, $[complex (l)]_0 = 1.0\times10^{-3}$ M, $[co\text{-}ligand (X)]_0 = 10.0\times10^{-3}$ M, $[PPA]_0 = 300.0\times10^{-3}$ M, $[H_2O_2]_0 = 100.0\times10^{-3}$ M) were chosen as optimal for comparative studies.

A series of co-ligands was tested to evaluate their effect on the catalytic performance. As summarized in *Table 1* and *Figure 3*, both the overall yields and the product distribution varied significantly with the nature of the co-ligand. Electron-withdrawing pyridine derivatives such as 4-cyanopyridine and 4-acylpyridines afforded the highest yields, while electron-donating ligands like 4-methylpyridine led to much lower conversion rates. Among heteroaromatic co-ligands, thiazole and benzothiazole were most active.

To obtain a more detailed picture of the electronic effects, a Hammett analysis was performed with para-substituted pyridines (*Figure 4*). A good linear correlation ($R^2 = 0.97$) with a positive reaction constant ($\rho = 0.59$) was obtained, suggesting that electron-withdrawing substituents accelerate the reaction by stabilizing the proposed high-valent iron–oxo intermediates and increasing their electrophilic character, thereby enhancing the reaction rate. This conclusion is further supported by electrochemical data. Cyclic voltammetry measurements revealed a clear relationship between the Fe(III)/Fe(II) redox potentials and the relative rate constants (*Table 2, Figure 5*) as well as with the product yields (*Figure 6*). In both cases, higher redox potentials were associated with enhanced catalytic activity. In the case of the relative rate constants, a linear relationship ($R^2 = 0.97$) with a gradient of m = 0.00136 indicates that higher redox potentials favor faster

Table 1: Effect of co-ligands on the H_2O_2 oxidation of 2-phenylpropionaldehyde catalysed by $[Fe(PBI)_3](OTf)_2$

Co-ligand (X)	$[1]_0$ ($\times10^{-3}$ M)	$[X]_0$ ($\times10^{-3}$ M)	$[PPA]_0$ ($\times10^{-3}$ M)	$[H_2O_2]_0$ ($\times10^{-3}$ M)	T (K)	Yield %	Yield $_{=O}$%	Yield $_{-OH}$%
Oxazole	1.0	10.0	300.0	100.0	293	18.0	12.6	5.4
Thiazole	1.0	10.0	300.0	100.0	293	24.3	17.0	7.3
Imidazole	1.0	10.0	300.0	100.0	293	8.0	5.5	2.6
Me-Imidazole	1.0	10.0	300.0	100.0	293	5.8	3.7	2.1
Benzoxazole	1.0	10.0	300.0	100.0	293	17.8	11.7	6.1
Benzothiazole	1.0	10.0	300.0	100.0	293	26.4	18.1	8.3
Benzimidazole	1.0	10.0	300.0	100.0	293	12.9	9.5	3.4
4-Me-Pyridine	1.0	10.0	300.0	100.0	293	9.5	8.2	1.4
Pyridine	1.0	10.0	300.0	100.0	293	14.4	10.7	3.7
4-PhC(O)-Pyridine	1.0	10.0	300.0	100.0	293	21.8	15.8	5.9
4-MeC(O)-Pyridine	1.0	10.0	300.0	100.0	293	25.4	18.1	7.3
4-CN-Pyridine	1.0	10.0	300.0	100.0	293	27.3	19.0	8.3

Table 2: Summary of the kinetic data for the H_2O_2 oxidation of 2-phenylpropionaldehyde catalysed by $[Fe(PBI)_2](OTf)_2$ in the presence of various co-ligands, including the Fe(III)/Fe(II) redox potentials ($E_{1/2}$ vs. Fc/Fc^+) and absorption maxima (λ_{max}) of the previously characterized $[(X)(PBI)_2Fe^{III}(\mu\text{-}O_2)Fe^{III}(X)(PBI)_2]^{4+}$ intermediate

Co-ligand (X)	$E_{1/2}$ (mV)*	λ_{max} (nm)*	k_{rel}
Oxazole	399	720	-
Thiazole	384	720	-
Imidazole	-265	670	-
Me-Imidazole	-255	670	-
Benzoxazole	467	715	-
Benzothiazole	399	712	-
Benzimidazole	53	698	-
4-Me-Pyridine	39	680	0.64
Pyridine	143	690	1.00
4-PhC(O)-Pyridine	332	720	1.58
4-MeC(O)-Pyridine	327	716	1.88
4-CN-Pyridine	407	728	2.05

reactions (*Figure 5*), while *Figure 6* shows that higher redox potentials are associated with increased product yields. The values represented in *Table 2* show that electron-withdrawing ligands shift the potentials towards more positive values and are associated with bathochromic shifts of the peroxo-intermediate absorption band.

Overall, these results demonstrate that the co-ligand environment plays a decisive role in modulating the efficiency and selectivity of non-heme iron catalysts in the oxidation of aldehydes. The combination of kinetic, spectroscopic and electrochemical studies highlights the strong influence of electronic effects in tuning the reactivity of these systems.

4. Discussion

Based on the kinetic, spectroscopic and electrochemical results, a plausible catalytic cycle can be proposed for the H_2O_2-mediated oxidation of 2-phenylpropionaldehyde. The reaction is initiated by the activation of hydrogen peroxide by the Fe(II) precursor complex. As suggested for related non-heme iron systems, two Fe(II) centers react with H_2O_2 to generate a *μ-1,2-peroxo*-diiron(III) intermediate. The spectroscopic feature observed at 720 nm can be assigned to such a *peroxo*-bridged species, which subsequently undergoes O–O bond cleavage.

Two mechanistic scenarios can be considered for the evolution of this intermediate. In one case, a high-valent *bis-μ-oxo*-diiron(IV) species, while in the other case, two mononuclear Fe(IV)=O species can be

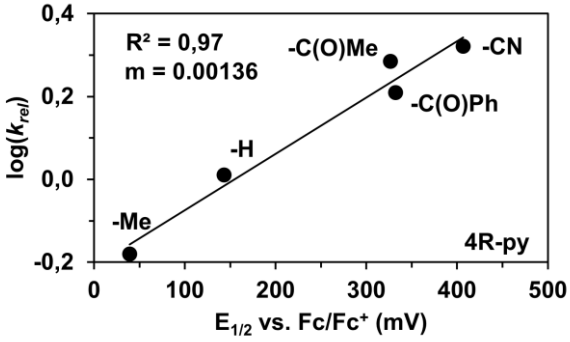

Figure 5: Correlation between the Fe(III)/Fe(II) redox potentials and the relative rate constants (k_{rel}) for the H_2O_2- oxidation of 2-phenylpropionaldehyde

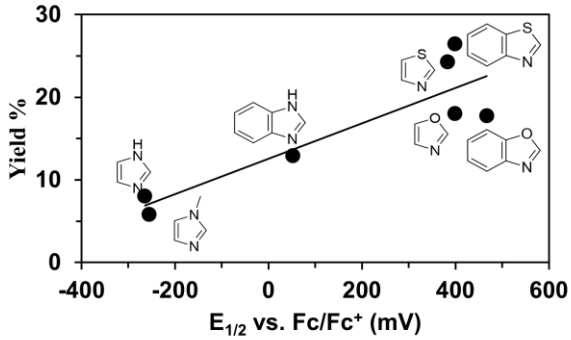

Figure 6: Correlation between the Fe(III)/Fe(II) redox potentials ($E_{1/2}$ vs. Fc/Fc^+) and the oxidation yields of 2-phenylpropionaldehyde in the presence of $[Fe(PBI)_3](OTf)_2$ with co-ligands containing different heteroatoms at 293 K

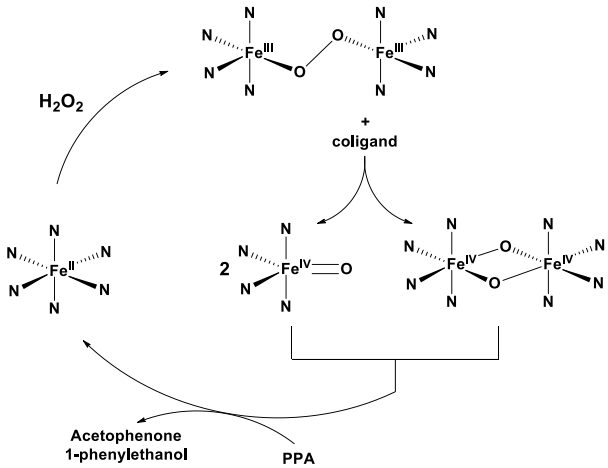

Figure 7: Proposed catalytic cycle for the H_2O_2-mediated oxidation of 2-phenylpropionaldehyde using $[Fe(PBI)_3](OTf)_2$ and co-ligands

regarded as the oxidation agent (*Figure 7*). Both pathways are plausible under the applied conditions and both generate oxidizing intermediates that are capable of hydrogen atom transfer (HAT) from the substrate. Such HAT steps initiate aldehyde oxidation, leading either to

deformylation and ketone formation or to hydroxylation of the benzylic position, resulting acetophenone and 1-phenylethanol, respectively, as oxidation products.

Following substrate oxidation, the iron center(s) are reduced back to Fe(II), thereby closing the catalytic cycle. The observed dependence of reactivity on the electronic properties of the co-ligands can be rationalized by considering that electron-withdrawing donors stabilize high-valent iron–oxo species, thus facilitating O–O bond cleavage and subsequent HAT reactivity. In contrast, electron-donating co-ligands disfavor such pathways, resulting in lower activity.

Together, these results highlight that the catalytic cycle likely involves a *μ-1,2-peroxo*-diiron(III) precursor that can evolve into either a *bis-μ-oxo*-diiron(IV) or two mononuclear Fe(IV)=O alternatives. Both intermediates are suitable in HAT chemistry and their relative contributions may depend on the co-ligand environment. This mechanistic flexibility is consistent with the observed ligand-dependent reactivity trends and emphasizes the crucial role of the co-ligand sphere in tuning the efficiency and selectivity of non-heme iron catalysts.

5. Conclusions

In this work, the influence of co-ligands on the H_2O_2-mediated oxidation of 2-phenylpropionaldehyde catalyzed by $[Fe(PBI)_3](OTf)_2$ was systematically investigated. Time-dependent studies revealed that the catalytic activity correlates with the decay of a *μ-1,2-peroxo*-diiron(III) intermediate, which is a key precursor in the catalytic cycle. By varying the co-ligand environment, significant differences were observed in both the reaction rates and product distribution. Electron-withdrawing substituents were found to accelerate oxidation and enhance product yields, as confirmed by *Hammett* correlations and redox potential measurements.

Mechanistic considerations suggest that the *peroxo* intermediate can evolve either into a *bis-μ-oxo*-diiron(IV) species or into two mononuclear Fe(IV)=O species, both of which are competent oxidants in hydrogen atom transfer. The results clearly demonstrate that the electronic nature of the co-ligand exerts a decisive influence on the efficiency and selectivity of non-heme iron catalysts. This study highlights the importance of fine-tuning ligand environments to modulate reactivity in biomimetic oxidation chemistry.

Acknowledgements

This research was funded by the University Research Fellowship Program (Code: 2024-2.1.1-EKÖP) of the Hungarian Ministry of Culture and Innovation, OTKA K142212 (J.K.) and TKP2021-NKTA-21 (J.K.) from the National Research, Development and Innovation Fund.

REFERENCES

[1] Howard, R.W.; Blomquist, G.J.: Ecological, behavioral, and biochemical aspects of insect hydrocarbons, *Annu. Rev. Entomol.*, 2005, **50**, 371–393, DOI: 10.1146/annurev.ento.50.071803.130359

[2] Schirmer, A.; Rude, M.A.; Li, X.; Popova, E.; Del Cardayre, S.B.: Microbial biosynthesis of alkanes, *Science*, 2010, **329**(5991), 559–562, DOI: 10.1126/science.118793

[3] Khara, B.; Menon, N.; Levy, C.; Mansell, D.; Das, D.; Marsh, E.N.G.; Leys, D.; Scrutton, N.S.: Production of propane and other short-chain alkanes by structure-based engineering of ligand specificity in aldehyde-deformylating oxygenase, *ChemBioChem*, 2013, **14**(10), 1204–1208, DOI: 10.1002/cbic.201300307

[4] Li, N.; Nørgaard, H.; Warui, D.M.; Booker, S.J., Krebs, C.; Bollinger Jr, J.M.: Conversion of fatty aldehydes to alka(e)nes and formate by a cyanobacterial aldehyde decarbonylase: cryptic redox by an unusual dimetal oxygenase, *J. Am. Chem. Soc.*, 2011, **133**(16), 6158–6161, DOI: 10.1021/ja2013517

[5] Hohenberger, J.; Ray, K.; Meyer, K.: The biology and chemistry of high-valent iron–oxo and iron–nitrido complexes, *Nat. Commun.*, 2012, **3**, 720, DOI: 10.1038/ncomms1718

[6] Friedle, S.; Reisner, E.; Lippard, S.J.: Current challenges of modeling diiron enzyme active sites for dioxygen activation by biomimetic synthetic complexes, *Chem. Soc. Rev.*, 2010, **39**(8), 2768–2779, DOI: 10.1039/C003079C

[7] Trehoux, A.; Mahy, J.-P.; Avenier, F.: A growing family of O_2 activating dinuclear iron enzymes with key catalytic diiron(III)-peroxo intermediates: Biological systems and chemical models, *Coord. Chem. Rev.*, 2016, **322**, 142–158, DOI: 10.1016/j.ccr.2016.05.014

[8] Kumar, R.; Pandey, B.; Sen, A.; Ansari, M.; Sharma, S.; Rajaraman, G.: Role of oxidation state, ferryl-oxygen, and ligand architecture on the reactivity of popular high-valent Fe^{IV}= O species: A theoretical perspective, *Coord. Chem. Rev.*, 2020, **419**, 213397, DOI: 10.1016/j.ccr.2020.213397

[9] Roy, L.: Theoretical identification of the factors governing the reactivity of C−H bond activation by non-heme iron(IV)-oxo complexes, *ChemPlusChem*, 2019, **84**(7), 893–906, DOI: 10.1002/cplu.201900178

[10] Mukherjee, G.; Alili, A.; Barman, P.; Kumar, D.; Sastri, C.V.; de Visser, S.P.: Interplay between steric and electronic effects: A joint spectroscopy and computational study of nonheme iron(IV)-oxo complexes, *Chem. Eur. J.*, 2019, **25**(19), 5086–5098, DOI: 10.1002/chem.201806430

[11] Mukherjee, G.; Lee, C.W.Z.; Nag, S.S.; Alili, A.; Reinhard, F.G.C.; Kumar, D.; de Visser, S.P.: Dramatic rate-enhancement of oxygen atom transfer by an iron(IV)-oxo species by equatorial ligand field perturbations, *Dalton Trans.*, 2018, **47**(42), 14945–14957, DOI: 10.1039/C8DT02142B

[12] Lakk-Bogáth, D.; Pintarics, D.; Török, P.; Kaizer, J.: Influence of equatorial co-ligands on the reactivity of $LFe^{III}OIPh$, *Molecules*, 2024, **29**(1), 58, DOI: 10.3390/molecules29010058

[13] Török, P.; Lakk-Bogáth, D.; Unjaroen, D.; Browne, W.R.; Kaizer, J.: Effect of monodentate heterocycle co-ligands on the μ-1,2-peroxo-diiron(III) mediated aldehyde deformylation reactions, *J. Inorg. Biochem.*, 2024, **258**, 112620, DOI: 10.1016/j.jinorgbio.2024.112620